Annals of the Academy of Romanian Scientists
Series on Science and Technology of Information
ISSN 2066 - 8562 Volume **3**, Number **2**/**2010**

TOWARDS NANO-SCALE RESONANT GAS SENSORS

Cornel COBIANU[1], Bogdan SERBAN[2], Violeta PETRESCU[3], Julia PETTINE[3], Devrez KARABACAK[3], Peter OFFERMAN[3], Sywert BRONGERSMA[3], Vladimir CHERMAN[4], Silvia ARMINI[4], Faezeh ARAB HASSANI[5], M.A. GHIASS[5], Yoshishige TSUCHIYA[5], Hiroshi MIZUTA[5], Cecilia DUPRE[6], Laurent DURAFFOURG[6], Alexandra KOUMELA[6], Denis MERCIER[6], Eric OLLIER[6], Dimitrios TSAMADOS[7] and Adrian M. IONESCU[7]

Abstract. *In this paper, we present preliminary results in the field of resonant Nano-Electro-Mechanical Systems (NEMS), where the gas/bio detection is performed by the frequency shift due to mass loading of the adsorbed analyte. The sensitivity of the resonant NEMS chemical sensors based on SOI-CMOSFET technology platform and a given sensor geometry is theoretically proven to be equal to 1 Hz/zeptogram in mass loading for the case of a novel detector circuit based on MOSFET transistor. The minimum frequency shift of 1 ppm is designed for the case of an readout consisting of a MEMS/NEMS based oscillator. Piezoresistive detection circuits performed in SOI-CMOSFET technology are also investigated due to their attractiveness for integrated resonant NEMS sensors. Surface functionalization for NO_2 detection with CNT moieties is described, in accordance with the HSAB theory. Also, localized functionalization with NH_2 self-assembled monolayer followed by biotin attachment or Au nanoparticles decoration is experimentally proven within SOI-CMOS technology. Novel reliability challenges due to Wan Der Waals and Casimir forces acting in the nanometer gaps between different parts are identified. Finally, the noise limitations for the minimum detectable mass in resonant NEMS are shown. The adsorption-desorption noise on the functionalized surface appears to be the most important, and this may be in agreement with the kinetic theory of gases giving us a first indication of the number collisions per second per our sensing surface, in the range of* $2 \cdot 10^9$.

Keywords: surface functionalization, resonant gas sensor, integrated NEMS, NO_2 detection

[1]Honeywell Romania, Sensors and Wireless Laboratory, Bucharest, Romania; corresponding member of The Academy of Romanian Scientists.
[2]Honeywell Romania, Sensors and Wireless Laboratory, Bucharest, Romania.
[3]Stichting IMEC, Eindhoven, The Netherlands.
[4]IMEC, Leuven, Belgium.
[5]University of Southampton, Southampton, United Kingdom.
[6]Laboratoire d'Electronique et de Technologie de l'Information, Grenoble, France.
[7]Ecole Polytechnique Fédérale de Lausanne, Suisse.

1. Introduction

The continuous miniaturization of the silicon integrated circuits (IC) has triggered a similar scaling down process for the sensing devices, as hardware interfaces for the real-time monitoring of the physical-chemical world. Thus, today, Micro-Electro-Mechanical Systems (MEMS) for acceleration and rotation velocity measurements are already an intrinsic part of cellular phones, portable video camera and home gadgets with wireless communication capabilities.

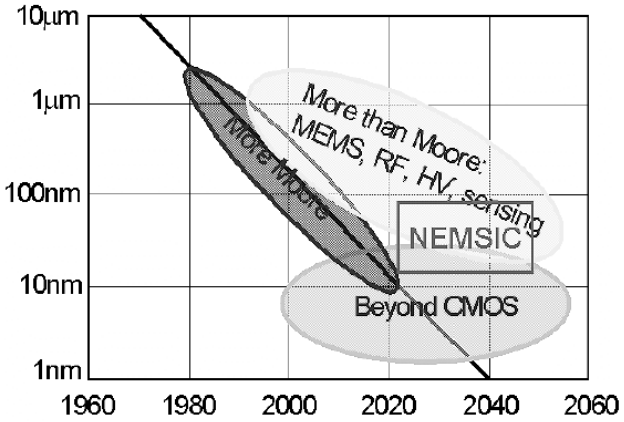

Fig. 1. "More Moore" in nanoelectronics and "More than Moore" in nanosensing will bring together Nano-Electro-Mechanical Systems and Integrated Circuit (NEMSIC) as ultimate integration phase in silicon technology.

With the electronic circuit integration going below 100 nm critical dimension, the nanoelectronics era started, and because the scaling down process has further followed the Moore law of scaling, with circuit complexity doubling every 12-15 months, it is generally accepted that nanoelectronics integration is included in the "More Moore" portion of the silicon technology roadmap. In the same time, there is also an intensive work to a more aggressive scaling down of the MEMS sensor to the nanometer scale, where mechanical, optical and bio-chemical nanosensors are emerging towards a novel family of nanosystems called Nano-Electro-Mechano-Systems (NEMS), as part of "More Than Moore" road map of the microsystems technologies (Fig.1) [1]. The ultimate stage of the silicon technology evolution is nearby, where the NEMS and integrated circuits (NEMSIC) are co-integrated on the same chip for the realization of the smart NEMS with multiple functionalities, and where electrical signal are coexisting with physical and chemical signal on the same chip. This NEMSIC era is shown in Fig.1 as a bridge between ultimate "More Moore" and "More Than Moore" stages and their monolithic integration on the silicon substrate.

Due to their nano-scale dimensions, the NEMS show high potential for sensitivities to forces in the range of Atto Newton (10^{-18} N), masses, in the range of Zepto grams (10^{-21} g), and heat capacities in the range of Yoctocalories (10^{-18} cal). Due to their reduced masses, the suspended nano-structures can also vibrate at high resonance frequencies and thus they offer a good potential for ultra-sensitive gas sensing by resonant principles. In this case of resonant gas nanosensors, the gas which is adsorbed on the vibrating beam is changing its overall mass and therefore its resonance frequency, which is thus indicative of the gas to be monitored. In the same time, as part of the nano-world, the performances of the nanosystems are limited by non-negotiable limits of the noise floor in both nanosensors and associated electronic circuits. The final performances of the nanosensors will be determined by both these expectations and limitations, which are deeply explored these days by the scientific community from all-over the world.

It is the purpose of this paper to show the early stage research results in the field of NEMS for resonant gas and bio sensing. The paper will describe the general principle of resonant gas nanosensors in the context of the SOI-CMOSFET technology. Then, the functionalization of the silicon surface for gas sensing will be shown in detail for the case of NO2 detection, as well as for biotin and gold nanoparticle functionalization. The on chip read-out circuit for the detection of the resonance frequency shift is presented. The reliability of the NEMS resonant is described at theoretical level. The paper will finally show the major noise sources in the resonant nanosensors, and their role in the minimum detectable mass by this principle.

2. Operation principle of resonant MEMS/NEMS gas/bio sensors

In this paper we shall describe the operation of the resonant gas/bio sensor by means of two approaches, which we call open loop and closed-loop configuration, depending on the system capability to track the changes in the resonance frequency of the vibrating beam.

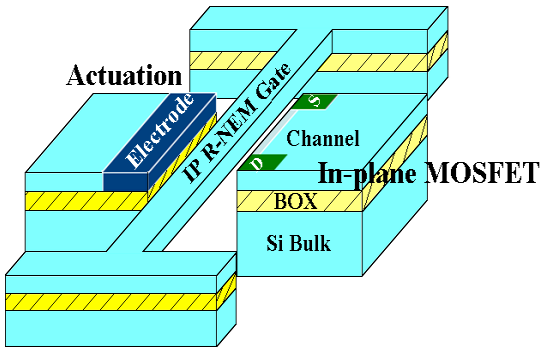

Fig. 2. In-plane resonant NEMS gas sensor,
with electrostatic actuation and MOSFET transistor detection.

2.1. Open-loop configuration.

The gas resonant sensors consists of an actuation circuit, a detection circuit and a vibrating suspended functionalized beam which is changing its resonance frequency as a function of the amount of gas/bio molecule to be detected. In Fig.2, we present a simple open loop configuration, where there is no feed-back loop between the detection and the actuation circuit so that the frequency of the actuation signal will not be automatically changed as a function of the changes in the mechanical resonance due to mass loading coming from the adsorbed gas to be detected by the sensor.

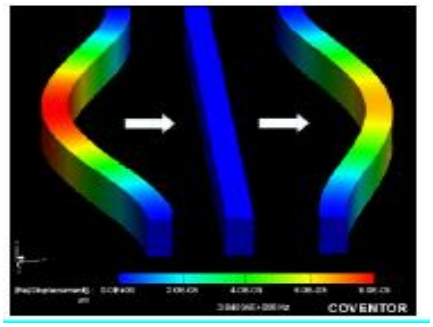

Fig. 3. In-plane vibration of the suspended gate, at its natural mechanical resonance frequency.

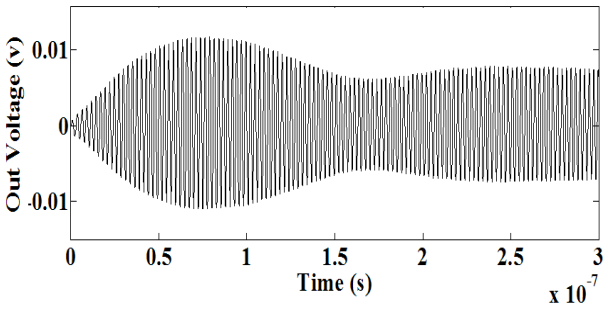

Fig. 4. Simulation of the transient response analysis of the open-loop resonant gas/bio nanosensor.

In addition, for this theoretical approach, the noise limitations are not included. The chemical functionalization of the surface of the vibrating beam is performed selectively, only on the vibrating beam surface, and the accreted mass due to gas/bio molecule adsorbed will be responsible for the shift of resonance frequency. In operation, the actuation circuit is applying an alternating excitation force which can be electrostatic, magnetic, thermal or piezoelectric, and whose frequency is equal with the natural mechanical resonance frequency of the vibrating beam. Such a condition for actuating the resonant beam can be simply expressed as below,

$$f_e = f_m \frac{1}{2\pi}\sqrt{\frac{k}{m}} \qquad (1)$$

where, f_e is the excitation frequency of the actuation signal, while, f_m is the mechanical resonance frequency, whose formula is written above. As shown in Fig. 2, the actuation is of electrostatic type, while a MOSFET transistor is used for the detection circuit, as originally proposed in [2,3] and based on optimization studies by the Southampton University research group. [4]. The operation of this NEMS resonant gas/bio sensor was simulated by Coventorware where the 3D modal analysis performed with Analyser module is presented in Fig. 3, where it is proven that the vibration is located in the horizontal plane. The suspended gate is vibrating at its mechanical resonance frequency. By setting the actuation ac

voltage to a frequency equal to the mechanical resonance of the vibrating beam, the in-plane oscillating gate will drive an ac drain current of the same frequency as the resonance frequency of the gate. Such a behavior was obtained in the Architect module of the Coventorware simulation. This drain current will flow through a load resistor which is providing the voltage response from Fig. 4. In this figure, we show the results of the Architect module, where the transient regime and the beginning of the steady state are displayed. The operation of the NEMS structure as a resonant gas sensor was simulated on this demo-structure by adding an ultrathin layer of material on the surface of the vibrating and tracking the frequency shift in the mechanical resonance frequency. Then, an ac signal of the same frequency was applied on the actuation side for driving the vibrating beam to that mechanical resonance frequency, and which at its turn is driving the drain current to oscillate at an electrical frequency equal to the mechanical frequency of the beam, which was initially shifted by the adsorbed gas/bio molecules. Such a theoretical demonstration model was able to detect an accretion mass equal to 1 attogram, with a sensitivity equal to 1 Hz/zeptogram . An alternative to resonant gate as detector circuit is the resonant-body MOSFET detection circuit, as proposed by EPFL research group [5-7].

2.2. Closed -loop configuration. MEMS/NEMS based oscillator

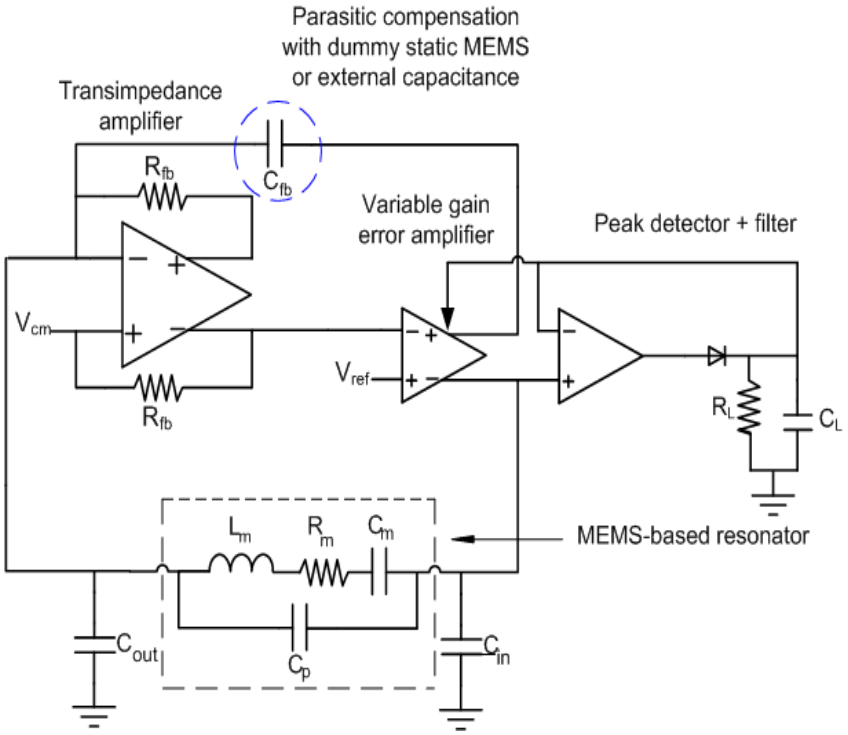

Fig. 5. Schematics of the MEMS/NEMS-based oscillator for gas/bio sensing applications.

In this case, the resonance frequency change due to the gas/bio molecule adsorbed on the vibrating micro or nano-beam is automatically detected by the electronic detection circuit, and therefore this configuration is applied in a real sensing application. Here, we show such an approach as it is developed by the Holst Centre from IMEC- The Netherlands, and where the entire electronic readout circuit for frequency shift monitoring of the MEMS/NEMS resonator is integrated on a single chip (Fig. 5).

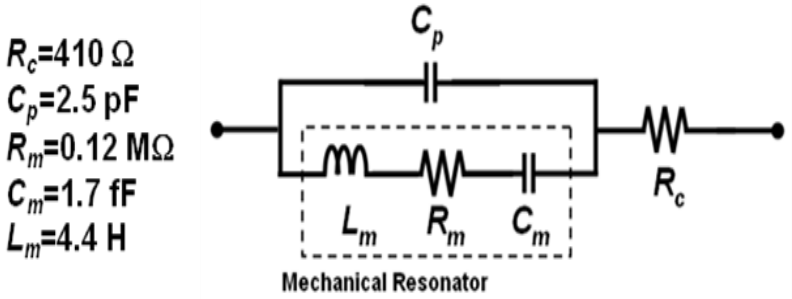

Fig. 6. Schematics of lumped-elements equivalent electric circuit of MEMS resonator vibrating at 1.8 MHz.

Simply speaking, this readout is an ultra high performance MEMS/NEMS based electronic oscillator, where the NEMS resonator (which can be made on a separate chip) is located in the feed-back loop of an electronic amplifier. The equivalent electrical circuit of the vibrating beam-based MEMS/NEMS resonator is represented by the well known Rm-Lm-Cm series circuit, which is specific to all second order vibrating electro-mechanical systems, and where the motional resistance, capacitance and inductance are determined by the material properties, geometry and technology of the vibrating beam and its interaction with the external ambient. At resonance, the vibrating beam will behave as an electrical resistance, which will act as a feed-back electric circuit for the electronic readout circuit. The mechanical resonance frequency of the vibrating beam and its shift as a function of the adsorbed gases on its surface will be read as an electronic signal frequency of the MEMS/NEMS based oscillator presented in Fig. 5.

In Fig. 6, we show the specific values of electric equivalent circuit of a MEMS resonator, which is obtained from a clamped-clamped vibrating beam with the vibration frequency of 1.8 MHz. The associated values of the RLC components are presented, together with the static capacitance (Cp) and series resistance Rc. For the above specified MEMS resonator, the transimpedance amplifier of the MEMS based oscillator from Fig. 5 will have the following characteristics:

- Loaded Q_L ~100
- Automatic gain control (AGC) with maximum allowed oscillation amplitude V_{osc}=100 mV (peak value)

- Resonator parasitic capacitance cancellation
- Amplifier bandwidth ≥ 10 × resonance frequency
- Phase noise (1 kHz) = – 78 dBc/Hz at 1.8 MHz resonance.

It is known that in MEMS-based oscillator circuits, in the case of driving oscillation amplitudes higher than a certain maximum value, the vibration of the beam could go beyond the linear (elastic) displacement regime and thus further generate non-linearity of the electric oscillation. To avoid these nonlinearities an automatic gain control circuit (AGC) was designed (see Figure 5). This circuit consists of a peak detector that measures the oscillation amplitude and its output is controlling an error gain amplifier that assures a closed loop gain of one.

The oscillator-based readout has been implemented in CMOS 0.25µm technology with 3.3 V supply voltage and consumes 1.6mW (buffer and bias included).

The simulation results obtained for the above MEMS based oscillator are shown in Fig. 7, where the time response at steady state regime is shown for the post-layout transient response based on the full chip parasitic extraction.

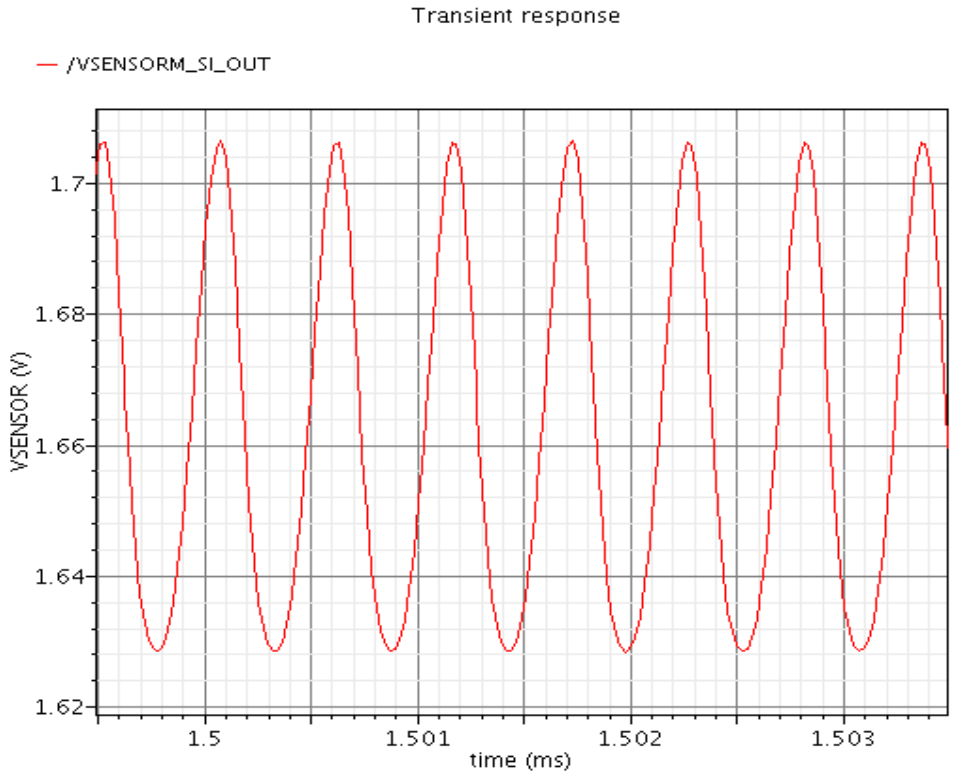

Fig. 7. Steady state response of the oscillator having a frequency of 1.8327 MHz and an oscillation amplitude of 77 mV.

As shown above, the resonator is electrically modeled using the lumped circuit: L_m, R_m, C_m. Based on the specifications of the phase noise, upper limits for the motional resistance are deduced. For example, for a resonator having a Q = 100 and an oscillator output voltage swing of 100 mV, a maximal motional resistance of 93 kΩ is allowed. According to the phase noise limitations of the sustaining amplifier, the input referred voltage noise should be limited to 0.133 nV/√Hz and the first stage transconductance has to be higher than 5.651×10^{-7} S.

The design rules deduced from the required mass resolution are necessary input specifications for the sensor and the analog IC. According to the simulation results, a phase noise limited at $L(f_m) = -77.37$ dBc/Hz at 1 kHz offset from the carrier frequency is achieved resulting in an equivalent minimum relative frequency shift $\delta f/f_{osc} = 10^{-6}$. This value will determine the minimum detectable mass and minimum detectable gas concentration, respectively, as it will be further explained in the next section.

As this readout is going to be used for real applications, which are targeting an accreted mass detection in the range of Atto (10^{-18}) to Zepto (10^{-21}) grams, a very detailed analysis of the circuit performances has to be performed. Thus, below the frequency stability and the noise response of the on-chip circuit are modeled and simulated.

2.3. Noise sources in an MEMS/NEMS oscillator-based readout system

The correlation of the oscillator phase noise with the mass resolution of the system through the Allan deviation was investigated and some results are presented here, as follows. To get a mass resolution in the order of attogram, an equivalent Allan deviation (frequency stability), as shown below is needed:

$$10^{-5} \le \frac{\delta f}{f_{osc}} \le 10^{-7} \tag{2}$$

For a NEMS resonator with a resonant frequency of f_{osc} = 150 MHz at an offset frequency, f_m = 1 kHz, the resonator intrinsic phase noise is

$$L(f_m) \le -60 dBc/Hz \tag{3}$$

and the system (oscillator and resonator) phase noise is:

$$L(f_m)_{\text{int}\,rinsic} \le -88 dBc/Hz \tag{4}$$

The noise sources in an oscillator based read-out are shown in Figure 8:

The resonator is modeled using the lumped circuit: Lm, Rm, Cm. Based on the specifications of the phase noise, upper limits for the motional resistance are deduced. For example, for a resonator having a Q=100 and an oscillator output

voltage swing of 100 mV, a maximal motional resistance of 93 kΩ is allowed. According to the phase noise limitations of the sustaining amplifier, the input referred voltage noise should be limited to 0.133 nV/√Hz and the first stage transconductance has to be higher than 5.651×10^{-7}S.

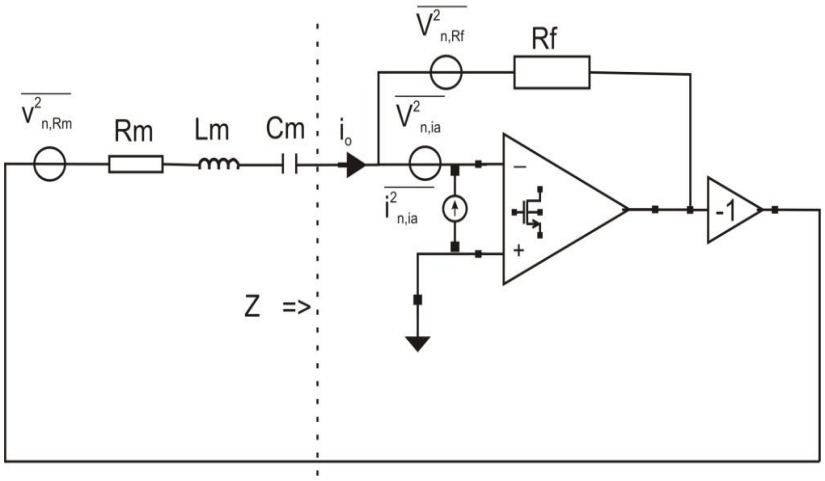

Fig. 8. Noise sources in an oscillator-based read-out system.

The design rules deduced from the required mass resolution are necessary input specifications for the sensor and the analog IC.

3. Functionalization for gas/bio sensing by NEMS resonators

3.1. Background of the functionalization for resonant NEMS sensing

One of the key advantages of the NEMS resonators is the large variety of types of gas and bio components that can be detected with high sensitivity and selectivity thanks to the vibrating beam functionalization that can be chemically designed for each species to be detected. To preserve the low mass of the NEMS vibrating beam in the range of (1-20) femptograms (fg) and below, and thus their excellent sensitivities, functionalized sensing monolayers should be grown on the surface of the beam [8]. If we consider a beam with the following dimensions: L = 2 μm, W = 100 nm and H = 40 nm, then we obtain a beam mass of 18 fg and with a surface area of $56\cdot10^{-10}$ cm^2. In order to understand which is the level of the mass loading due to the gas/bio component adsorbed on the functionalized surface, we are presenting below, in Fig. 8, the generic stages of a gas sensing process where we start from clean silicon surface having about 10^{15} dangling bonds, and continue with Si surface modification to generate Si-OH groups on the surface, to which we are linking the monolayers provided with gas sensing terminal groups noted by Y in our figure. In our generic example from below we shall consider that the gas to be detected is NO_2.

If we are considering a simple scenario where the yields η1, η2 and η3 of the surface modification, functionalization and sensing, respectively are all equal to 0.5, then the mass loading the silicon beam due to NO2 gas detection on the above functionalized surface area would be

$$\delta_m = 5.3 \cdot 10^{-17} \text{ g} \tag{5}$$

From the theory of the NEMS resonators, for the above assumptions, one can calculate the frequency shift associated to the mass increase due to adsorbed gas, as follows [9]:

$$\boxed{\frac{\delta m}{m} = \frac{5.3 \cdot 10^{-17}}{1.8 \cdot 10^{-14}} = 3 \cdot 10^{-3} = 2\delta f \,/\, fo} \tag{6}$$

The electronic read-out described above can measure with good accuracy such a mass loading, and even much lower accreted masses due to gas adsorbed on the functionalized vibrating beam. The challenges may appear if the gas concentration in the ambient is very low, below ppm's, and the associated mass loading is giving a frequency shift which is below the minimum frequency shift that can be detected by the electronic read-out. (In this case, the mass loading cannot be detected due to noise floor of the detection system).

An important step in understanding the limits of the gas/bio detection by resonant NEMS principle is related to the relation between the concentration of the gas/bio component in the ambient and the mass loading associated to the detection process for that concentration in the surrounding. Static calculations of the number of NO_2 molecules being hosted on the functionalized sensing surface, in the case of 1 ppm of NO_2 in the ambient is quite low, due to ultra small sensing surface, but this static approach may not fit well the dynamic processes of gas molecules collisions with the sensing surface. If we consider the kinetic theory of gases, then we are closer to the real dynamic process of gas molecule hitting randomly the surface of the functionalized beam, as follows. The total number of collisions (A) of air molecules per unit time per area is:

$$A = \frac{\rho}{4}\sqrt{\frac{8kT}{\pi m}}. \tag{7}$$

where, ρ is the air density, m is the mass of the air molecule in kg, k is Boltzmann constant, T is absolute temperature. By doing these calculation for the case of air molecules, we get $A=3 \cdot 10^{27}$ collisions per second per m2. If we consider the area of the functionalized sensing beam from above, the total number of collisions will be about $2 \cdot 10^{15}$ per second, and finally, if we remember that the NO_2 concentration is 1 ppm, then we get about $2 \cdot 10^{9}$ NO_2 molecules collisions per second per our sensing area. Such NO_2 collisions events are at the origin of the selective reactions between the functionalized surface and NO_2 molecules, which will finally generate the accreted mass needed for the resonant detection.

3.2. Functionalization for NO2 sensing by resonant NEMS

Carbon Nano Tubes (CNT) were chosen as sensing layer for NO_2 detection in accordance with the principle of the hard soft acid base (HSAB) theory.

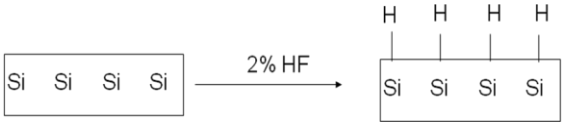

Fig. 9. Silicon surface hydrogenation by treatment in diluted HF.

The sequence of the chemical processes for the silicon surface functionalization with CNT is presented below [10]. In the first step, the native oxide is removed by means of silicon wafer rinsing in diluted HF silicon, and surface hydrogenation is the obtained as, shown in Fig. 9. The hydrogen terminated Si wafer is then exposed to a stream of ozone so that the Si-H bonds are replaced by Si-OH bonds, as shown in Fig. 10.

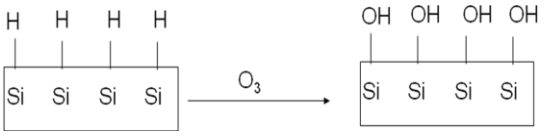

Fig. 10. Hydroxyl terminated silicon surface prepared by ozone treatment in diluted HF.

In the next step, the OH terminated wafer is treated in amino alcohol for a time and temperature enough to produce an amino (NH_2) terminated silicon surface as shown in Fig. 11. The Si wafers are then cleaned in alcohol, deionzed water and dried in N_2.

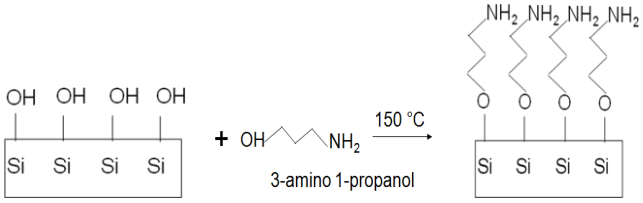

Fig. 11. Amino terminated silicon surface prepared by amino alcohol treatment.

Separately, an amount of carbon nanotubes (CNT) is sonicated in a mixture of nitric acid and sulfuric acid at a suitable ratio, frequency, power and duration sufficient to functionalize one or more CNT with a carboxilic group as shown in Fig. 12.

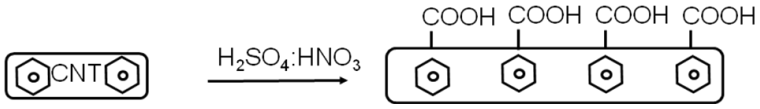

Fig. 12. CNT functionalized with carboxylic groups in diluted HF.

In the next stage, these functionalized CNT are mixed with thionil chloride ($SOCl_2$) so that to convert the carboxilic acid moities to carboxilic chrloride moities, COCl-CNT, as shown in Fig. 13.

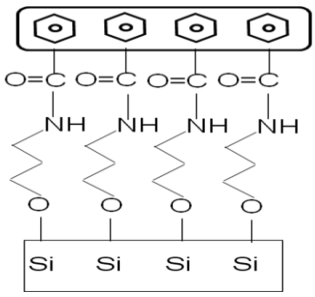

Fig. 13. CNT functionalized with carboxylic chloride groups.

These CNT-COCl are reacting then with the silicon substrate having the NH_2 terminated surface (see Fig. 11), in order to obtain the silicon surface functionalized with CNT moities for NO_2 detection, as shown in Fig. 14.

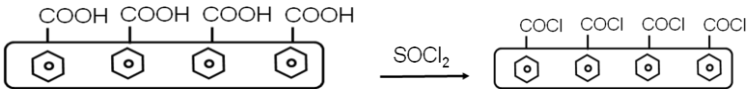

Fig. 14. CNT terminated silicon surface for NO2 detection.

The entire functionalized process described above should happen selectively, on the surface of the future vibrating beam, which act as NO_2 detection region in the resonant NEMS sensor.

3.3. Functionalization for bio-sensing with resonant NEMS

Here, we show an example of silicon nanowire functionalization for biosensing applications, where Joule heating ablation is used for selective functionalization [11]. This selective process is performed in a sequence of steps, as shown below (Fig. 15).

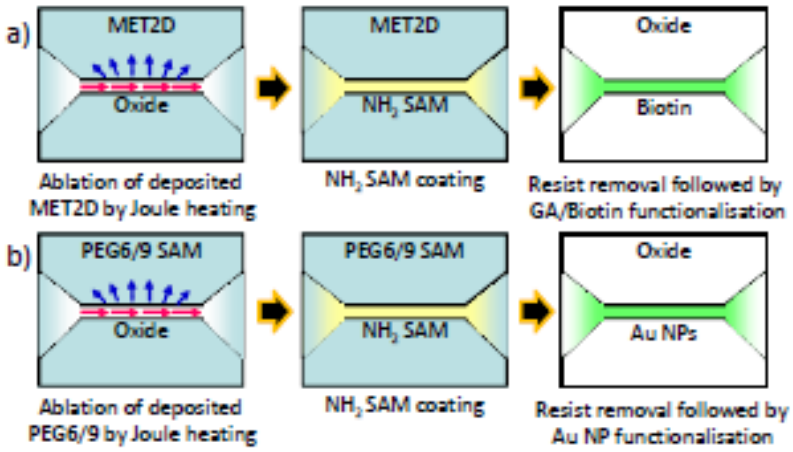

Fig. 15. Functionalization of Si nanowire with biotine (a) or with Au nanoparticles (Au NP) (b) in diluted HF

Initially the Si nanowires are processed on the Si wafer by standard IC technology, and then the entire Si wafer is covered with a 100 nm thick photoresist layer. The photoresist covering the Si nanowire is selectively removed by the local Joule heating generated by an electrical current flowing through the doped Si nanowire. After a short UV-ozone cleaning step, the entire wafer is functionalized with an amino self-assembled monolayer (NH_2-SAM). In the following step, the photoresist is removed in acetone without affecting the NH_2-SAM functionalized Si nanowire. The NH_2 groups are further selectively bio-coupled with biotin through glutaraldehyde cross-linker (Fig. 15 a) or "decorated" with gold nanoparticles (Au NP) (Fig. 15 b). The silicon surface modification is influencing the electrical properties of the Si nanowires, in the direction of minimizing the temperature dependence of the electrical conductivity, as proved elsewhere [11].

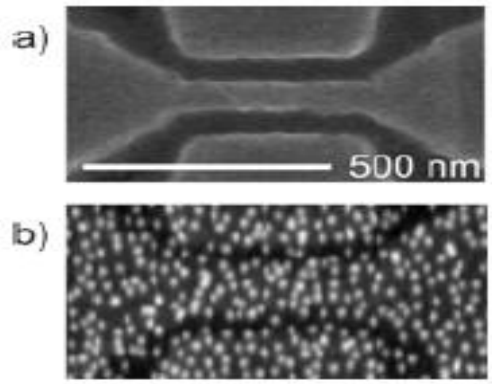

Fig. 16. Si nanowire before (a) and after (b) Au NP functionalization.

4. SOI-CMOSFET compatible technology for resonant NEMS gas sensors

The SOI-CMOSFET technology platform is expected to play an important role for both NEMS resonator realization as well as electronic circuit for signal processing from the sensor. The release of the suspended silicon nanobeam can be easily performed in the SOI technology by the selective etching of the buried SiO_2 layer between the Si film and the silicon substrate, and this is a key process for the fabrication of the NEMS structures. IC-SOI-CMOSFET compatible fabrication of the suspended nanobeams will assure the on-chip integration of both resonant sensor and its electronic circuit for driving and detecting the resonance frequency and its shift as a function of accreted mass on the vibrating beam, and this is an emerging technology for smart resonant NEMS sensing. Among multiple possibilities of the detection of the frequency of the vibrating beam, the piezoresistive behavior of the silicon vibrating beam can be used as an attractive IC compatible approach. In Fig. 17, a SEM picture of a suspended silicon nanowire performed in the fully depleted SOI-CMOSFET technology of CEA-LETI laboratory is shown.

The key processes for the realization of piezoresistive nanobeam are doping control, e-beam lithography, Si plasma etching and Si beam release.

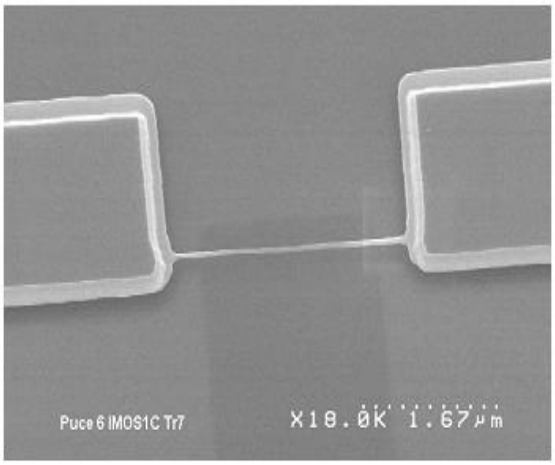

Fig. 17. Suspended Si nanowire obtained in SOI-CMSFET technology.

In Fig. 18, we show the electrical resistance of the piezoresistive nanowire as a function of the length of the nanobeam. The linear dependence of the resistance is passing closed to the origin of the axes from Fig. 18 proving a small contact resistance of the piezoresistor made by the above technology.

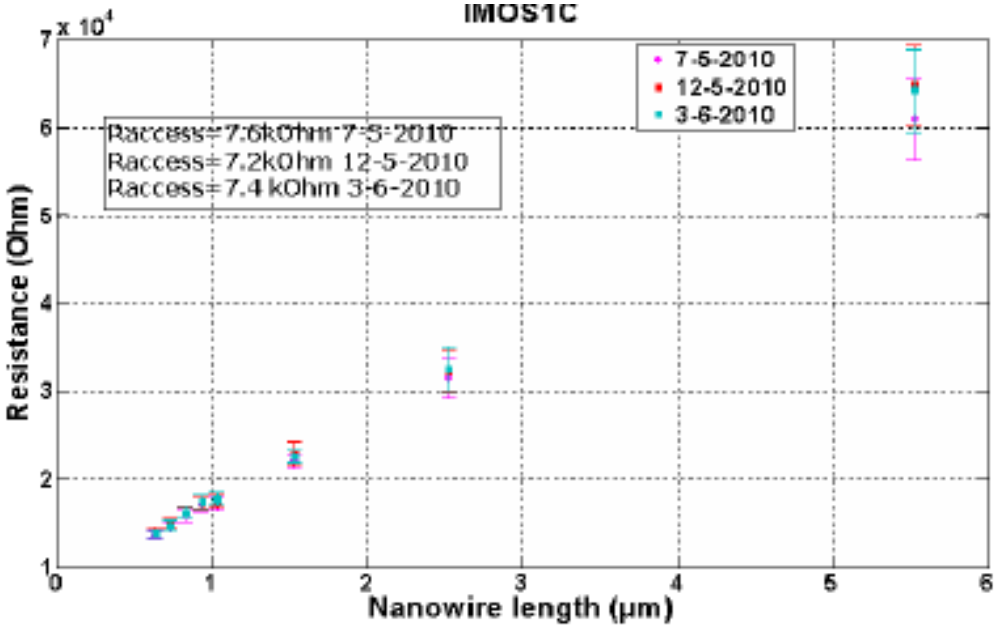

Fig. 18. Electrical resistance of the piezoresistive nanowire performed in the SOI-CMoSFET technology.

The high value of the piezoresistor of about 70 kΩ for a length of 7 μm is indicating some of the future challenges of the piezorestive semiconductor nanoresonators in terms of impedance mismatch between sensor and amplifier, higher flicker noise and high temperature dependence [12].

5. Reliability of the resonant NEMS gas sensors

The reliability of the SOI-CMOSFET NEMS gas sensors is an important topic in the early stage of their research and development, as this is revealing the potential roadblocks of the present technologies. These days, one of the key issues with the resonant nanosensors is the identification and control of the forces acting on the vibrating beam due to the fabrication process and the operation of the biased sensor. Thus, the following forces have been found to influence the reliable operation of the resonant NEMS sensors:

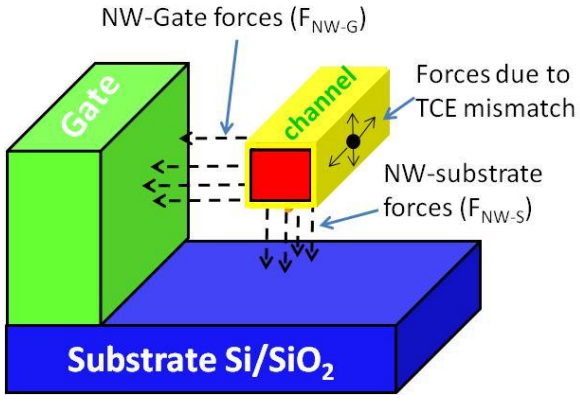

Fig. 19. A diagram showing the forces developed between vibrating gate and surrounding substrate and actuating gate in SOI-CMOSFET structures.

Electrostatic "Channel-to-Gate" force, which is a "useful" force, as it assures the actuation of the vibration beam for reaching and maintaining its mechanical resonance condition.

Electrostatic "Channel-to-substrate" force, which is not a useful force, and therefore the biasing of the substrate should be done in such a way, so as to avoid such electrical forces between the vibrating beam and substrate.

Thermo-mechanical forces due to the mismatch of the thermal coefficients of the expansion (TCE) of different materials constituting the device. These forces are not useful and they should be minimized by selecting the proper type of materials and their geometries for sensor realization. In Fig. 20, a SEM picture of a suspended silicon beam performed in the NEMS platform of EPFL laboratory is shown. In this figure one can see the silicon beam buckling out of horizontal plain, as a result of thermo-mechanical forces developed between the beam and its clamping ends.

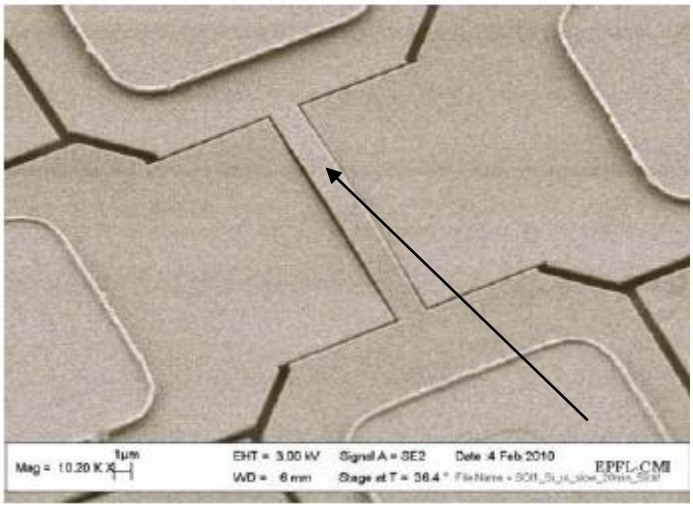

Fig. 20. A diagram showing the Si beam buckling, out of horizontal plane, for small gaps between the vibrating gate and actuating gate in SOI-CMOSFET structures.

Mechanical restoring (spring) forces in the nanowire, which are useful elastic forces resulting from the conversion of the mechanical kinetic energy of the vibrating beam into potential energy and vice versa.

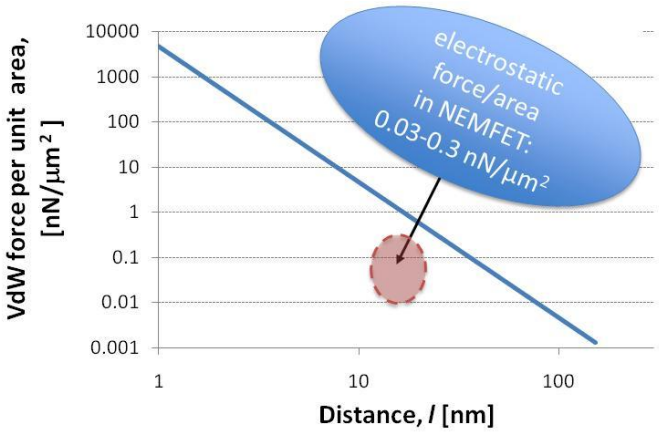

Fig. 21. Theoretical results of Van Der Waals forces between SiO_2 plates, in vacuum, as a function of nanometer gap.

Van Der Waals and Casimir forces, which are not useful forces, but they will be acting between nanosystem components, when the distance between them is in the range of nanometers. From quantum mechanics point of view, they represent the effect of the zero-point fluctuations of the electromagnetic waves in the nano-electro-mechanical devices. In Fig. 21 we show an important theoretical result, where it can be seen that for the case of SiO_2 semi-infinite plates, placed in vacuum, and separated by an ultra small gap in the range of few tens of

nanometers, the Van Der Waals force can be higher than the electrical forces specific to NEMS –SOI-CMOSFET sensors. This theoretical value means that these forces cannot be ignored when we design the resonant nanosensors.

One of the key reliability issues of the resonant NEMS-SOI-CMOSFET sensors for gas detection is coming from the need to expose the MOSFET transistor to the ambient to be monitored and still requiring a stable transistor operation. This will further trigger an intense research effort to passivate the silicon surface, like in the early stages of MOSFET technology, so that humidity and electrostatic charges to have a minimum impact on the transistor threshold voltage and thus not to influence the stable IV characteristics of the MOSFET transistor.

6. Noise limits in resonant NEMS sensors

The sensing performance in the nanoworld is inexorably limited by the noise mechanisms [13], [14]. This is also the case of the nanoresonators for mass detection [9, 15, 16].

As described by Cleland and Roukes [15] and Ekinci et al. [9,16], the fundamental noise sources in a double clamped nanooscillator are thermomechanical noise, temperature fluctuation noise, adsorption-desorption noise and momentum exchange noise.

In the sensing regime, the nanocantilever works as a dumped mechanical oscillator due to the ambient atmospheric air surrounding which opposes to its movement. On the other side, in the termodynamical equilibrium, the medium returns the oscillator the energy lost by dumping [17]. This produces a random mechanical motion of the small object, a phenomenon known as thermomechanical noise.

This phenomenon is a direct consequence of the fluctuation-dissipation theorem. Due to its finite thermal conductance, the temperature of the nanoresonator fluctuates. These fluctuations are translated into the frequency fluctuations and are known as temperature fluctuation noise. The adsorption-desorption noise is due to environmental molecules which are adsorbed-desorbed on and from the nanoresonator surface. The molecules mass load the resonator and, in effect, modify the resonance frequency. Random fluctuations in the adsorbtion-desorption process produce fluctuations (noise) in the resonance frequency.

The ambient molecules impinging on the nanoresonator surface exchange momentum with it [9,16]. This generates fluctuations of the resonant frequency (momentum exchange noise). Momentum noise is practically absent in the vacuum. Depending on the experiment purposes, all these mechanisms can act as fundamental limits in mass sensing. They are well documented in the literature, and their intensity can be analytically calculated and compared [9,15,16].

It would be of interest to compare and predict what would be the dominant noise limit in our NEMSIC resonator. To this purpose, we estimated the volume of our nanoresonator: $V=8x10^{-12}$ mm^3. Therefore, log (V, mm^3) is about -11.

From the dependence of the quality factor (Q) vs. log (V, mm^3) (see [9], Fig. 7), one can deduce a Q value of about 10^3. Assuming this value for Q, one can easily observe from the calculated data of Ekinci et al. [16] that the limit for mass sensitivity due to thermomechanical noise (δM_T) is higher than that imposed by temperature fluctuation noise.

To compare the contribution of the thermomechanical noise with that of momentum noise, we deduced from [16] that the ratio of the mass sensitivity determined by thermomechanical noise (δM_T) and momentum exchange noise (δM_M) is $\delta M_T/\delta M_M=(Q_{gas}/Q)^{1/2}$, where Q_{gas} is the quality factor due to gas dissipation and Q is the intrinsic (unloaded) quality factor of the resonator. It is clear that the momentum exchange noise becomes dominant when $Q>Q_{gas}$.

For nanoresonators with high Q, the momentum noise becomes increasingly important for molecules with higher mass (m) because $Q_{gas}\sim(m)^{-1/2}$. However, obtaining a high Q for a resonator with log (V) ≈ -11 is difficult because this factor indicates an extremely high surface-to-volume ratio.

Therefore, the dissipation mechanisms in our resonator are surface controlled. It results that a Q of about 1000 cannot be easily obtained. Even with passivation layers, lower values are to be expected.

At room temperature and atmospheric pressure, absorption-desorption noise appears to be the most important limit for the mass sensitivity of the nanoresonators [9, 15-17]. Djuric et al. [18] numerically compared the external noise limits and found that for resonator beams with resonant frequency between 100 kHz and 10 GHz, the adsorbtion-desorption noise is higher than the thermomechanical and temperature fluctuation noise. Moreover, according to their calculation [11], the adsoption-desorption noise, at room temperature, increases by five orders of magnitute when the desorption energy of the gas molecule varies from 10kcal/mol to 16kcal/mol. This indicates that the sensitivity of the nanoresonator to a given gas molecule could be imposed by the noise level induced by other (ambient) molecules which strongly bound to the sensor surface.

On the other side, since the desorption of a strongly bounded gas molecule generates more noise, it results that the molecule impedes on its detection by itself! These are factors of challenge in both nanoresonator and sensing experiments design.

A problem which is not discussed in the literature is related to the effect of the functionalization layer on the noise mechanisms in nanoresonator.

For instance, the surface termination strongly affects the mechanical energy dissipation [19] and this is not due to a mass loading effect but to a chemical one.

Consequently, the quality factor and, implicitly, the associated noise mechanisms can be strongly affected by the molecular scaffold used for functionalization. Also, it is not clear at all what happens with the surface dissipation mechanisms in the presence of functionalization layer: are they passivized or not?

All these are important challenges for the realization of a reliable nanoresonator.

7. Conclusions

The resonant SOI-CMOSFET NEMS gas/bio sensors represent an important fundamental research topic and an emerging technology for many applications, thanks to the high flexibility offered by the surface functionalization methods which can tailor sensing layers for a large variety of chemical detectors.

The results on modeling and simulation of operation principle of the resonant NEMS with SOI-CMOSFET transistor as a detection circuit have shown that a mass loading sensitivity of the order of 1 Hz/zeptogram can be obtained.

An important step forward towards an integrated resonant NEMS gas/bio sensor is performed by driving and reading the frequency of the resonant sensor by placing it in the feed-back loop of a transimpedance amplifier which is provided with control of maximum oscillation amplitude for avoiding non-elastic displacement of the vibrating beam. With such a MEMS/NEMS-based oscillator, a relative frequency shift of 1 ppm can be detected, which will assure high sensitivities gas/bio detection, at the benefit of an on-chip read-out circuit for signal processing.

The paper has shown the entire chemical process of the surface functionalization for the NO2 detection with CNT moities, as well as the IC compatible technology for the selective functionalization of the silicon nanowire with gold nanoparticles or biotin, which are decorating the NH2 self-assembled monolayers, previously deposited on the nanowire.

SOI-CMOSFET technology is used as an integrated platform for the fabrication of NEMS resonant sensor, as well as the circuit for signal processing from the sensor, where the piezoresistive detection is envisaged.

At the nanometer scale, novel reliabilities challenges are identified in NEMS resonant sensors, where the Wan Der Waals and Casimir forces between plates separated by nanometer gaps could be higher than the actuation electrostatic forces.

An intensive research will be needed for the passivation of the silicon surface of the sensing SOI-CMOSMOSFET resonant devices, which have to be exposed directly to the ambient to be monitored, and thus may be influenced by the humidity and electrostatic charge, affecting their electrical stability.

The noise mechanisms in resonant NEMS sensors are thoroughly investigated in our paper, as they will provide the ultimate sensitivity limits of the nanotechnology-based chemical detection. In good agreement with the above results of the kinetic theory indicating a number of about $2 \cdot 10^9$ collisions per second per a sensing surface of $56 \cdot 10^{-10}$ cm^2, it is shown that at room temperature and atmospheric pressure, absorption-desorption noise appears to be the most important limit for the mass sensitivity of the nanoresonators.

This work is creating a robust foundation for the understanding the major challenges in the realization of the NEMS resonant chemical sensors and the technology roadmap for the next generation of integrated SOI-CMOSFET NEMS chemical sensors.

Acknowledgments

This paper is supported by EU-FP-7 NEMSIC project and Honeywell International.

REFERENCES

[1] Adrian M. Ionescu, "Nano Electro-Mechanical-Systems: from Idea to Reality Check" in New Developments in Micro-Electro-Mechanical Systems for Radio Frequency and Millimeter Wave Applications, pp 91-96, 2009, Editura Academiei Romane, ISBN 978-973-27-1813-1.

[2] Durand, C.; Casset, F.; Renaux, P.; Abele, N.; Legrand, B.; Renaud, D.; Ollier, E.; Ancey, P.; Ionescu, A.M.; Buchaillot, L.; In-Plane Silicon-On-Nothing Nanometer-Scale Resonant Suspended Gate MOSFET for In-IC Integration Perspectives IEEE Electron Device Letters, Volume: 29 , Issue: 5 2008, pp. 494 - 496.

[3] Colinet, E.; Durand, C.; Duraffourg, L.; Audebert, P.; Dumas, G.; Casset, F.; Ollier, E.; Ancey, P.; Carpentier, J.-F.; Buchaillot, L.; Ionescu, A.M.; Ultra-Sensitive Capacitive Detection Based on SGMOSFET Compatible With Front-End CMOS Process IEEE Journal of Solid-State Circuits, , Volume: 44 , Issue: 1, 2009, pp. 247 - 257.

[4] F. A. Hassani, C. Cobianu, S. Armini, V. Petrescu, P. Merken, D. Tsamados, Adrian M. Ionescu, Y. Tsuchiya, and H. Mizuta, Design and Analysis of an In-Plane Resonant Nano-Electro-Mechanical Sensor for Sub-Attogram-Level Molecular Mass-Detection, Extended Abs. Int. Conf. on Solid State Devices and Materials 1332 (2009).

[5] D. Grogg, M. Mazza, D. Tsamados, A. M. Ionescu, "Multi-Gate Vibrating-Body Field Effect Transistors (VB-FETs)", IEDM 2008, San Francisco, USA, 15-17 December 2008.

[6] D. Grogg, S. Ayoz, A. M. Ionescu, "Self-sustained low power oscillator based on vibrating body field effect transistor", IEDM 2009, Baltimore, USA, 07-09 December 2009.

[7] D. Grogg, A. Lovera, A. M. Ionescu, "Nano-Electro-Mechanical Vibrating Body FET Resonator for High Frequency Integrated Oscillators", DRC 2010, South Bend, USA, 21-23 June, 2010.

[8] Cornel Cobianu, Bogdan Serban, Mihai Mihaila, Viorel Dumitru, Faezeh A. Hassani, Yoshishige Tsuchiya, Hiroshi Mizuta, Vladimir Cherman, Ingrid De Wolf, Violeta Petrescu, Juan Santana, Cecilia Dupre, Eric Ollier, Thomas Ernst, Philippe Andreucci, Laurent Duraffourg, Dimitrios Tsamados and Adrian Ionescu, Nano Scale Resonant Sensors for Gas and Bio Detection: Expectations and Challenges, Proceedings of CAS 2009 Conference, p. 259.

[9] K.L. Ekinci and M.L. Roukes, "Nanoelectromechanical systems", in Review of Scientific Instruments, vol. 76, 061101 (2005).

[10] Bogdan Serban, Cornel Cobianu, Mihai Mihaila, Viorel Dumitru, "Functionalization methods for NO_2 detection by all differential nanoresonators", Filing date: 12/11/2009

[11] M. A. Ghiass, S. Armini, M. Carli, A. Maestre Caro, V. Cherman, J. Ogi, , S. O da, Z. Moktadir, Y. Tsuchiya, and H. Mizuta, Temperature insensitive conductance detection with surface-functionalised silicon nanowire sensors. In: 36th International Conference on Micro- and Nano-Engineering (MNE) 2010, 19 to 22 September 2010, Genoa, Italy.

[12] Mo LI, H.X. Tang and M.L. Roukes, "Ultrasensitive NEMS based cantilevers for sensing, scanned probes and very high frequency applications", in Nature Nanotechnology, Vol 2, Feb 2007, pp 114.

[13] M. N. Mihaila, 1/f Noise in Nanomaterials and Nanostructures: Old Questions in a New Fashion, in Advanced Experimental Methods for Noise Research in Nanoscale Electronic Devices, J. Sikula and M. Levinshtein (Eds.), Kluwer Academic Publisher, pp. 19-27, 2004.

[14] Mihai N. Mihaila, Cornel Cobianu, Cleopatra Cabuz, From micro- to nanosensors: do we need paradigm changes?, in Instrumentation and Metrology for Nanotechnology, Report of the National Nanotecnology Initiative Workshop, NIST, Gaithersburg, January 27-29, pp. 143-144, 2004; http://www.nano.gov/NNI_Instrumentation_Metrology_rpt.pdf.

[15] A. N. Cleland, M. L. Roukes, Noise processes in nanomechanical resonators, J. Appl. Phys. 92, pp. 2758-2769, 2002.

[16] K. L. Ekinci, Y. T. Yang and M. L. Roukes, Ultimate limits to inertial mass sensing based upon nanoelectromechanical systems, J. Appl. Phys. 95, pp. 2682-2689, 2004.

[17] Yook Kong Yong, John Vig, Resonator surface contamination- A cause of frequency fluctuations? IEEE Trans. Ultrason., Ferroelect. Freq. Contr. 36, pp. 452-458, 1989

[18] Z. Djuric, O. Jaksic, D. Randjelovic, Adsoption-desorption noise in micromechanical resonant systems, Sensors and Actuators A 96, pp. 244-251, 2002.

[19] Yu Wang, Joshua A. Henry, Debodhonyaa Sengupta and Melissa A. Hines, Methyl monolayers suppress mechanical energy dissipation in micromechanical silicon resonator, Appl. Phys. Lett. 85, pp. 5736-5738, 2004.